

Electrochemical lithium ion intercalation in $\text{Li}_{0.5}\text{Ni}_{0.25}\text{TiOPO}_4$ examined by *in situ* X-ray diffraction

Rickard Eriksson ^{a,*}, Kenza Maher ^b, Ismael Saadoune ^b, Mohammed Mansori ^b, Torbjörn Gustafsson ^a, Kristina Edström ^a

^a Department of Materials Chemistry, The Ångström Laboratory, Uppsala University, Box 538, SE, 751 21 Uppsala, Sweden

^b University Cadi Ayyad, FST Marrakech, LCME, Av. A. Khattabi, BP549, Marrakech, Morocco

ARTICLE INFO

Article history:

Received 9 September 2011

Accepted 1 November 2011

Available online 2 December 2011

Keywords:

Batteries

Lithium intercalation compounds

In situ X-ray powder diffraction

ABSTRACT

The complex structural transformations of $\text{Li}_{0.5}\text{Ni}_{0.25}\text{TiOPO}_4$ during electrochemical lithiation have been examined by *in situ* X-ray diffraction. During the first lithiation two structural changes take place: first a transition to a second monoclinic phase ($a = 9.085(4)$, $b = 8.414(5)$, $c = 6.886(5)$, $\beta = 99.85(4)^\circ$) and secondly a transition to a third phase with limited long-range order. The third phase is held together by a network of corner sharing Ti–O octahedra and phosphate ions with disordered Ni–Li channels. During delithiation the third phase is partially transformed back to a slightly disordered original phase, $\text{Li}_{0.5}\text{Ni}_{0.25}\text{TiOPO}_4$ without formation of the second intermediate phase. These phase transitions correspond well to the different voltage plateaus that this material shows during electrochemical cycling.

© 2011 Elsevier B.V. All rights reserved.

1. Introduction

There is constantly a hunt for new electrode materials for lithium-ion batteries. New cathode materials could lead to batteries with higher energy densities and new anode materials could lead to better safety. Therefore, oxyphosphates have in recent years attracted attention for their use as lithium intercalation materials in the voltage range around 1.5 V vs. Li/Li^+ . The first oxyphosphate material reported as electrode material was $\text{Ni}_{0.5}\text{TiOPO}_4$ [1]. This was later followed by $\text{Co}_{0.5}\text{TiOPO}_4$ [2]. An *in situ* X-ray diffraction study of $\text{Ni}_{0.5}\text{TiOPO}_4$ was performed by Maher *et al.* and they observed an irreversible peak broadening of the parent phase during the first discharge, which was accompanied by the appearance of a new phase which was stable during the following cycling [3]. The $\text{Li}_{0.5}\text{Ni}_{0.25}\text{TiOPO}_4$ oxyphosphate was first synthesized by Manoun *et al.* [4] and it was recently studied as negative electrode material in a lithium-ion battery [5,6].

In this study, the detailed structure of $\text{Li}_{0.5+x}\text{Ni}_{0.25}\text{TiOPO}_4$ ($0 < x < 1.5$) as a function of lithium content is presented. This material has a theoretical capacity of 225 mAh/g if the Ni^{2+}/Ni and $\text{Ti}^{4+}/\text{Ti}^{3+}$ redox couples are fully involved. However, when cycled between 3.0 and 0.5 V a capacity of 300 mAh/g is obtained during the first discharge and about 200 mAh/g during subsequent charge/discharge cycles. During the first discharge, the voltammogram of the studied

material shows three distinct peaks: 1.43 V, 1.24 V and 0.80 V [5]. The capacity of the first peak is the largest (147 mAh/g) and it was suggested by Maher *et al.* that this voltage plateau corresponds to the reduction of Ti^{4+} to Ti^{3+} . However, Hollmark *et al.* [6] showed the reactions to be more complicated by the use of resonant inelastic X-ray scattering and X-ray absorption spectroscopy. The change in oxidation state of the Ti ions is not linear with the amount of intercalated lithium: it has a minimum (highest electron occupation in 3d-band) at the 1.43 V plateau, to reach a local maximum at the fully discharged state, and then during charging the 3d-band will again be filled. The change in oxidation state for Ni was shown to be a change from Ni^{2+} at $x=0$ (0 mAh/g), to Ni^+ at $x=1.5$ (225 mAh/g) and to metallic Nickel at $x=2.0$ (300 mAh). During the consecutive first charge, the Ni is not changed back to Ni^{2+} but only to Ni^+ . During the full cycle of the material the oxygen ions do also participate to some extent in the charge uptake in the material, but the spectroscopic results showed this to happen at the very end of the discharge (during the 0.8 V peak, where also the SEI is formed). Hollmark *et al.* conclude that this material does not have a clear and linear oxidation process, but rather a lot of “cross-talk” between the different atomic species (Ni, Ti and O).

In this study, we have examined $\text{Li}_{0.5+x}\text{Ni}_{0.25}\text{TiOPO}_4$ by *in situ* X-ray diffraction to monitor the material response to electrochemical lithiation and to examine if the well defined voltage plateaus are due to crystalline to crystalline transitions. The well defined voltage plateaus might indicate that this material has more crystalline order than has been reported for the intercalation of lithium into $\text{Ni}_{0.5}\text{TiOPO}_4$ [3].

* Corresponding author.

E-mail address: rickard.eriksson@mkem.uu.se (R. Eriksson).

2. Experimental

$\text{Li}_{0.5}\text{Ni}_{0.25}\text{TiPO}_4$ was synthesized from a stoichiometric mixture consisting of an aqueous solution of LiNO_3 (99%, Aldrich), $\text{Ni}(\text{NO}_3)_2 \cdot 6\text{H}_2\text{O}$ (99%, Aldrich), and $(\text{NH}_4)_2\text{HPO}_4$ (98%, Merck) with a solution of TiCl_4 (99% Aldrich) diluted in ethanol. Addition of the titanium solution to the aqueous mixture with constant stirring, at room temperature, induces the formation of precipitates. The solvents were evaporated at 45°C under vacuum, the resulting powder was heated in air at 400°C for 12 h and then at 900°C for 12 h [5]. The product was examined by powder neutron diffraction at the GEM-beamline at ISIS facility at Rutherford Appleton Laboratory, UK.

Electrodes were made with a composition of 75% active material, 10% carbon black (Super P) and 15% PVDF. The slurry mixture was ballmilled for 2 h and the slurry was then casted on an aluminium foil and dried at 60°C for 2 h; the resulting electrodes had an average active material loading of 2.0 mg/cm^2 . Electrodes were cut from the foil and dried in a vacuum furnace inside an argon filled glovebox ($\text{O}_2, \text{H}_2\text{O} < 2\text{ ppm}$) for 5 hours at 120°C . Pouch cells were then assembled inside the glovebox with a Li counter electrode, Solupor separator and a 1 M LiPF_6 EC:DEC 2:1 electrolyte.

In situ X-ray diffraction was measured at beam line I711 at the MAXlab synchrotron in Sweden (wavelength 1.003 \AA). The samples were mounted in transmission mode geometry and an Oxford Titan CCD was used to collect diffraction pattern with the detector at different 2θ angles. The dataset was reduced with CrysAlis-software to xy-powder-patterns covering 5 to 84° in 2θ . The diffraction patterns were collected while the battery was electrochemically cycled with a current of C/10 (calculated for 225 mAh/g), using an Autolab potentiostat.

In house *in situ* X-ray diffraction experiments were also done on a STOE diffractometer with a position sensitive detector and the sample in transmission mode with $\text{Co K}\alpha_1$ radiation (wavelength 1.789 \AA). The cell was discharged in steps for 6 h at C/30 with intermittent stops for diffraction pattern collection. The cells were assembled as for the synchrotron experiments but with a different electrolyte (1 M LiClO_4 EC/DEC 2:1) and a Celgard separator.

3. Results and discussion

The neutron diffraction experiments showed a highly crystalline starting material. Rietveld refinement (Fullprof software [7]) of the neutron powder diffraction data gave cell parameters (Space group: $P2_1/c$, $a = 6.4012(5)$, $b = 7.2635(5)$, $c = 7.3684(6)$, $\beta = 90.388(7)$, $R(\text{Bragg}) = 13.2$, $R_f = 6.33$) in good agreement with literature [4]. This refined model was used as starting model for all the XRD refinements. This 3D structure consists of an open framework favourable for lithium intercalation. It contains three-dimensional networks of TiO_6 and NiO_6 octahedra and PO_4 tetrahedra within which lithium ions are located. Each TiO_6 octahedron shares one face with one NiO_6 octahedron, while NiO_6 octahedron shares corners with four PO_4 tetrahedra and two other corners with two TiO_6 octahedra. Lithium atoms fully occupy the site 2a, whereas nickel atoms occupy statistically half of the site 2b. The Ti^{4+} ions are isolated in the structure. This explains why the electronic conductivity (hopping mechanism) is low in this phosphate.

Fig. 1 shows the cycling performance of the cell used for the *in situ* synchrotron diffraction experiment (current rate C/10, calculated from theoretical capacity). There is a big polarization in the cell as compared to earlier published results [5,6], the capacity of the material is also lower and the expected voltage plateaus are smeared and not clearly visible.

In Fig. 2 diffraction patterns from the synchrotron experiment are shown. The first part of the lithium insertion into $\text{Li}_{0.5}\text{Ni}_{0.25}\text{TiPO}_4$ up to 2 h results in a directional solid solution behaviour (starting material indicated as “A” in Fig. 2). This insertion of lithium results

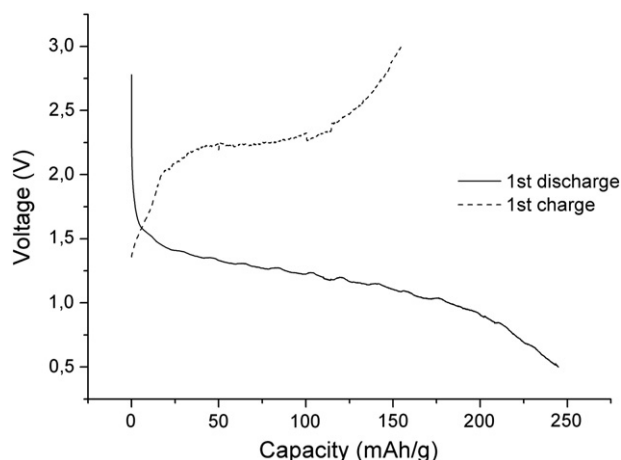


Fig. 1. First discharge and charge cycle for $\text{Li}_{0.5}\text{Ni}_{0.25}\text{TiPO}_4$ vs. Li at C/10 rate. First discharge (solid) and first charge (dashed).

in an increase in the *a*-cell parameter, while the *b* and *c* directions are almost unaffected as seen by the shifts in $(2\ 0\ 0)$, $(2\ 1\ 1)$ and $(-2\ 1\ 1)$ but not in $(0\ 1\ 2)$ and $(0\ 2\ 2)$. However, already at 2 h (Fig. 2) a phase transition is starting which is clearly observable at 6 h. The new peaks (indicated “B”) can be indexed by a monoclinic unit cell (Table 1). Continued lithiation shows a continued two phase reaction. After 8 h the two phases still coexists but after 10.5 h the peaks from the starting phase have vanished completely. Also the peaks from the second phase have disappeared and a set of new weak and broad peaks can be seen (marked “C”). This might indicate a second phase transition to a third phase during the first discharge.

Dominating in the diffraction peak is the strong peak around 17.56 degrees, in the starting material this is the $(0\ 1\ 2)$ -peak (d-spacing 3.28 \AA). During the lithiation this peak shifts to longer d-values and loses intensity. At “C”-phase this d-spacing is about 3.33 \AA .

During delithiation (charging from 10.5 h to 20 h) it is not until 18 h a transformation back to the original phase without a transformation to the intermediate phase is observed. The peak positions and the peak-half widths are indicating strain and or coherent domain

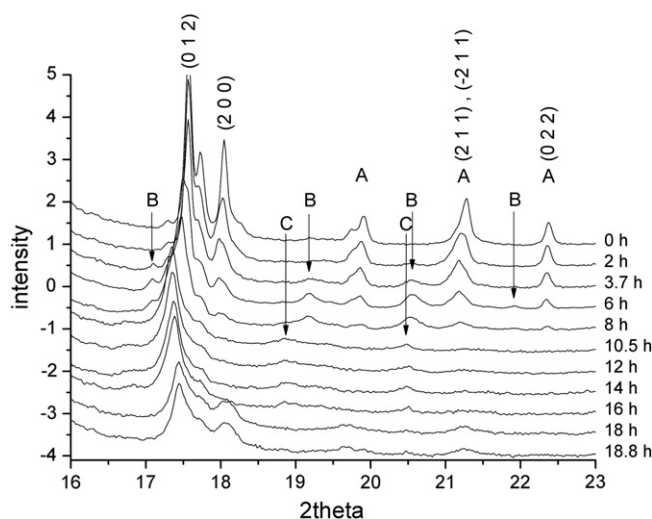


Fig. 2. Diffraction pattern collected at different times during the first *in-situ* discharge-charge cycle (C/10) of $\text{Li}_{0.5}\text{Ni}_{0.25}\text{TiPO}_4$ vs. Li/Li^+ . The discharge is between 0 h to 10.5 h, and then the sample is charged. Capital letters indicate features in the diffraction patterns: A is the starting material (with indices for some peaks marked), B indicates a first set of new peaks and C indicates a third set of peaks. Intensities for the different diffraction patterns have been scaled to the background intensity (at 22.74 deg).

Table 1

Cell parameters of the original phase $\text{Li}_{0.5}\text{Ni}_{0.25}\text{TiOPO}_4$ (marked as “A” in table and figures), refined from the *in situ* experiments diffraction patterns. The new peaks (indicated “B” in Fig. 2) present at 6 h can be indexed by a monocline unit cell (Phase B).

Time(h)	Phase	a	b	c	beta	Bragg R
0	A	6.397(2)	7.259(4)	7.366(3)	90.31(8)	13.4
6	A	6.413(3)	7.287(6)	7.393(4)	90.41(11)	51.1
6	B	9.085(4)	8.414(5)	6.886(5)	99.85(4)	
End	A	6.392(18)	7.275(40)	7.423(21)	90.79(93)	52.4

length modifications. Cell parameters for the original phase at 0 h, 6 h and at the end of experiment is shown in Table 1.

In Figs. 3 and 4 the results from the in-house *in situ* X-ray diffraction experiments are displayed. Fig. 3 shows the electrochemistry (C/30) from the first discharge with intermittent stops where the diffraction experiments were performed. This experiment at low discharge rate show the capacity of the material with good agreement with previously reported data [5,6].

In Fig. 4 diffraction patterns recorded every fifth hour from the C/30 discharge are depicted, where the original ($\text{Li}_{0.5}\text{Ni}_{0.25}\text{TiOPO}_4$) phase is present from 0 to 15 h but not in the patterns at 25 h and at the end of the experiment. At 15 h there are also new diffraction peaks (marked “B”) from the same intermediate monoclinic phase as seen midway into the synchrotron experiments. However, at the end of the experiment (30 h) this second phase has disappeared completely. The diffraction pattern from the end of discharge has only one visible reflection, corresponding to the strongest peak in the synchrotron diffraction pattern collected at 10.5 h. This strengthens the assumption that a third phase is formed at the end of the discharge process. In this case the lithiation process was carried out slower than in the synchrotron study and at each position in the discharge curve the sample was allowed to equilibrate.

When comparing the results to that of Hollmark et al. [6] there are some interesting observations to be made: they report nonlinearity in the occupancy of the Ti 3d-band with a maximum occupancy at the 1.43 V plateau coexisting with the first new phase appearing in the diffraction pattern in our experiment. Later there is a change in the Ni oxidation state which might be coupled to the appearance of the second new phase and the 1.24 V plateau.

Fig. 5 shows the crystal structure of $\text{Li}_{0.5}\text{Ni}_{0.25}\text{TiOPO}_4$ viewed down the a-axis. Half-occupied Ni-sites (grey) and lithium sites (green) form edge sharing channels in the a-direction. Between these channels are infinite ribbons (in the a-direction) of corner sharing

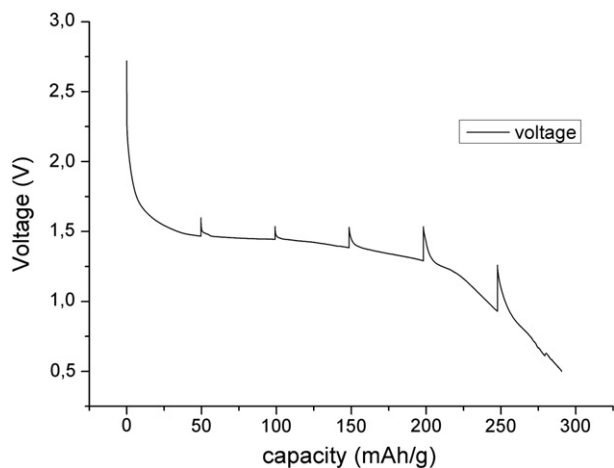


Fig. 3. First discharge at C/30 rate for $\text{Li}_{0.5}\text{Ni}_{0.25}\text{TiOPO}_4$ vs. Li/Li^+ for the in-house *in situ* X-ray diffraction experiments. The figure is displaying the discharge-stops where overnight diffraction experiments were recorded. Selected diffraction results are available in Fig. 4.

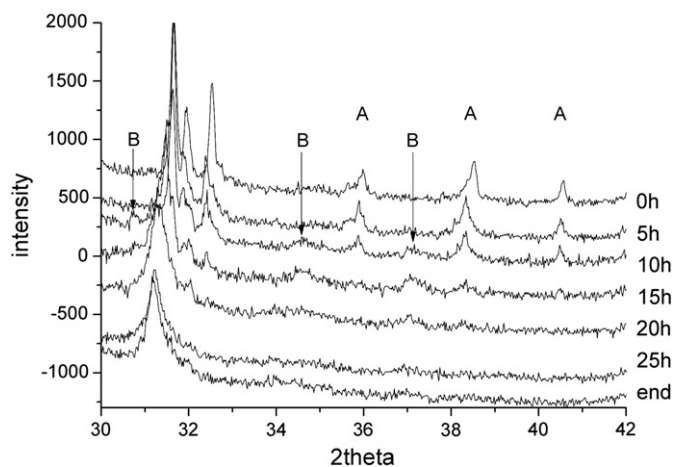


Fig. 4. Diffraction pattern collected at different times during the first discharge (C/30) of $\text{Li}_{0.5}\text{Ni}_{0.25}\text{TiOPO}_4$ vs. Li/Li^+ for the in-house *in situ* XRD experiment. At 15 h there are new diffraction peaks indicating a first order phase transition in the *in situ* experiments. A second phase transition occurs at the end of discharge, leaving virtually only one observable diffraction peak. Capital letters indicate features in the diffraction patterns: A is the starting material, B indicates a first set of new peaks.

Ti-octahedrons (blue) and phosphate-tetrahedrons (purple). These ribbons are normal to the (0 1 2) direction forming an open titanium-phosphate network. Parallel ribbons are also linked by face sharing Ni–Ti octahedrons and oxygen bridging ions.

Reduction of the Ti-ions will increase the Ti–O bond length leading to an expansion along the a-direction (parallel to the infinite ribbons) as seen in the solid solution range between 0 and 2 h in the synchrotron data. Further change in the Ti-oxidation state will result in the formation of a new crystalline phase (“B”). A change in the oxidation

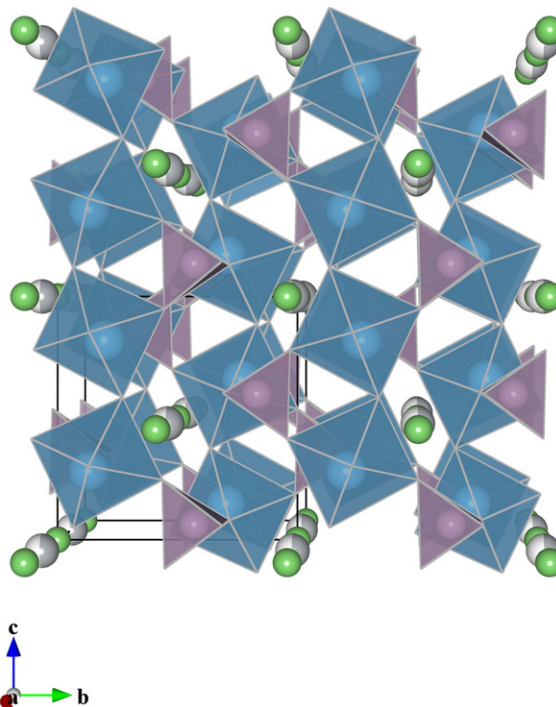


Fig. 5. Crystal structure of $\text{Li}_{0.5}\text{Ni}_{0.25}\text{TiOPO}_4$ viewed down the a-axis. Half-occupied Ni-sites (grey) and lithium sites (green) form edge sharing channels in the a-direction. Between these channels are sheets (in the a-direction) of corner sharing Ti-octahedrons (blue) and phosphate-tetrahedrons (purple). There exists two separate sets of sheets, parallel to two crystallographic planes, the (0 1 2) and (0 1 -2). Sheets parallel to each other are interconnected by face sharing Ti–Ni octahedron, and sheets of different sets are interlocked by sharing Ti-octahedrons.

state of Ni will not only give a bond length (Ni–O) expansion but might lead to a weakening of the bonding between the Ti–PO₄ ribbons. This will result in some disorder but with the Ti–PO₄ framework keeping the long range order in the stacking direction. This leads to a formation of phase “C”. A further change in Ni oxidation state to Ni⁰ coupled with a change in the oxidation state of oxygen [6] will further decrease the binding attractions in the crystal between the Ti–PO₄ ribbons, resulting in more disorder and a lower crystallinity (Fig. 4). However, since the Ti–PO₄ ribbons also are linked to each other, this framework will still be intact resulting in diffraction peaks at d-values of their spacing (in the order of 3.3 Å).

During the following charge (delithiation, 12 h to 18.8 h in synchrotron experiment) there is a shift of the 3.33 Å peak towards smaller d values (12 to 16 h) and then a rapid appearance (16 h to 18h) of a new set of peaks corresponding to the original phase “A.” The existence of only one plateau in the voltammogram during the charge [5] is consistent with the existence of only two phases during the charge process as in Fig. 2. The reduced crystallinity in the “A” phase after one complete discharge–charge cycle is consistent with the result of a only partial oxidation of Ni during charge (to Ni⁺) [6] if explained by the Ti–PO₄ ribbons being more loosely bound to each other by a Ni⁺ than by Ni²⁺.

4. Conclusions

The complex structural transformations in Li_{0.5}Ni_{0.25}TiOPO₄ during lithiation have been revealed with *in situ* X-ray diffraction. Two new phases have been observed during the first lithiation: a second

monoclinic lithium rich phase and then a third phase with limited long-range order. The second phase is held together by a network of corner sharing Ti–O octahedra and phosphate ions with disordered Ni–Li channels. The third phase is during the following charge partially transformed back to a slightly disordered original phase Li_{0.5}Ni_{0.25}TiOPO₄ without formation of the second intermediate phase.

Acknowledgements

We are grateful for the opportunities we have had to work at the MAXIV laboratory synchrotron facility in Lund, Sweden, and all the technical support we have received from their wonderful staff. This work was financially supported by the Swedish Energy Agency and the Swedish Research Council (VR). StandUp for Energy is also recognised for support.

References

- [1] I. Belharouak, K. Amine, *Electrochem. Commun.* 7 (2005) 648–651.
- [2] R. Essehli, B. El Bali, H. Ehrenberg, I. Svoboda, N. Bramnik, H. Fuess, *Mater. Res. Bull.* 44 (2009) 817–821.
- [3] K. Maher, K. Edström, I. Saadoune, T. Gustafsson, M. Mansori, *J. Power Sources* 196 (2011) 2819–2825.
- [4] B. Manoun, A. El Jazouli, P. Gravereau, J.P. Chaminade, *Powder Diffr.* 17 (2002) 290–294.
- [5] K. Maher, K. Edström, I. Saadoune, T. Gustafsson, M. Mansori, *Electrochim. Acta* 54 (2009) 5531–5536.
- [6] H.M. Hollmark, K. Maher, I. Saadoune, T. Gustafsson, K. Edström, L.-C. Duda, *Phys. Chem. Chem. Phys.* 13 (2011) 6544–6551.
- [7] J. Rodriguez-Carvajal, *Physica B* 192 (1993) 55–69.